Geostandards and Geoanalytical Research
September 2021, Volume 45 Issue 3 Pages 525-538
https://doi.org/10.1111/ggr.12378
https://archimer.ifremer.fr/doc/00684/79594/

Silicon Isotope Analyses of Soil and Plant Reference Materials: An Inter- Comparison of Seven Laboratories

Delvigne Camille [1, 2, *], Guihou Abel [1], Schuessler Jan A. [3, 4], Savage Paul [5], Poitrasson Franck [6], Fischer Sebastian [5], Hatton Jade E. [7], Hendry Katharine R. [7], Bayon Germain [8], Ponzevera Emmanuel [8], Georg Bastian [9, 10], Akerman Alisson [6], Pokrovsky Oleg S. [6, 11], Meunier Jacques [1], Deschamps Pierre [1], Basile-doelsch Isabelle [1]

[1] Aix Marseille Univ ,CNRS IRD, INRAE, Coll. France, CEREGE, Europôle Méditerranée de l'Arbois BP 80 13545 Aix-en-Provence cedex ,France
[2] Earth and Life Institute Environmental sciences, Université Catholique de Louvain L7.05.10 1348 Louvain-la-Neuve, Belgium
[3] Thermo Fisher Scientific ,Bremen ,Germany
[4] GFZ,German Research Centre for Geosciences Potsdam 14473 ,Germany
[5] School of Earth & Environmental Sciences University of St Andrews Irvine Building, St Andrews, KY16 9AL, UK
[6] Géoscience and Environment Toulouse (GET), UMR 5563 CNRS-University of Toulouse III-IRD-CNES 14 Avenue Edouard Belin 31400 Toulouse ,France
[7] School of Earth Sciences ,University of Bristol Wills Memorial Building, Queens Road Bristol, UK
[8] IFREMER, Marine Geosciences Unit Brest,France
[9] Water Quality Center Trent University ,Peterborough ON K9L 1Z8 ,Canada
[10] Agilent Technologies Canada, 6705 Millcreek Dr Mississauga ON L5N 5M4 ,Canada
[11] BIO-GEO-CLIM ,Laboratory Tomsk State University Lenina av., 36 Tomsk, Russia

* Corresponding author : Camille Delvigne, email address : camille.delvigne@uclouvain.be

Abstract :

The use of silicon (Si) isotopes has led to major advances in our understanding of Si cycling in modern and past environments. This inter-laboratory comparison exercise provides the community with the first set of soil and plant reference materials with an analytically challenging matrix containing organic material that is known to induce isotopic bias, for use as secondary reference materials in Si isotope measurement. Seven laboratories analysed four soil reference materials (GBW-07401, GBW-07404, GBW-07407, TILL-1) and one plant reference material (ERM-CD281). Participating laboratories employed a range of chemical preparation methods and analytical setups but all analyses were performed by MC-ICP-MS. Irrespective of the chemical preparation method or analytical conditions, the results show excellent agreement among laboratories within 2s for at least three replicates. Data were combined together to calculate δ29Si and δ30Si mean values (relative to NBS 28) and their expanded uncertainties (U, coverage factor k = 2). The δ30Si values are as follow: GBW-07401: -0.27 ± 0.06 ‰, GBW-07404: -0.76 ± 0.12 ‰, GBW-07407: -1.82 ± 0.17 ‰, TILL-1: -0.16 ± 0.06 ‰ and ERM-CD281: -0.28 ± 0.11 ‰. Also, a compilation of published data provides an up-to-date mean δ30Si for BHVO-2 of -0.28 ± 0.08 ‰.

Keywords : silicon isotopes, reference materials, soil, plant, inter-comparison of measurements

Silicon (Si), the second most abundant element in the Earth's crust, is a ubiquitous rock-forming element and is considered as a key component of global biogeochemical cycles, due to links with

carbon cycling and other nutrient systems. Chemical weathering of silicate minerals controls atmospheric CO_2 concentration and thus regulates climate over geological timescales (e.g., Berner *et al*. 1983). Silicate weathering also releases dissolved Si into the hydrosphere, and thereby ultimately controls the biological pump, because Si is an essential nutrient in marine and freshwater ecosystems (Nelson *et al*. 1995, Ragueneau *et al*. 2006). Although the oceanic Si cycle has been a key research focus for decades, the terrestrial Si cycle has attracted increasing scientific attention after the important and complex role of vegetation was recognised (Conley 2002, Street-Perrott and Barker 2008, Struyf and Conley 2012). Processes occurring at the land-ocean interface and anthropogenic impacts are now actively studied using Si isotopic variations or "fingerprints" (Engström *et al*. 2010, Hughes *et al*. 2011, 2013, Vandevenne *et al*. 2015, Mangalaa *et al*. 2017).

Silicon has three stable isotopes: ^{28}Si, ^{29}Si and ^{30}Si with mean relative isotope abundances of 92.23%, 4.67% and 3.10%, respectively (Barnes *et al*. 1975, De Bièvre and Taylor 1993). Pioneering Si isotope investigations in natural systems showed the potential to provide better understanding of the biogeochemical cycle of Si in both modern and past environments (see Basile (2006) for an early review). However, studies remained limited because of sometimes hazardous, but often delicate and time-consuming analytical methods. The advent of MC-ICP-MS instruments, combined with improved sample preparation techniques (e.g., Georg *et al*. 2006), have subsequently allowed Si isotope measurements to flourish and led to great advances in our understanding of the global Si cycle (see Poitrasson (2017) for a more recent review).

For analyses, matrix-matched reference materials (RMs) are required to allow inter-laboratory comparisons and to check for data quality for everyday analytical work – particularly in systems where calibrator-sample bracketing is the traditional way to measure isotope ratios. To date, only three inter-laboratory comparisons have been published for Si isotopes (Reynolds *et al*. 2007, Hendry *et al*. 2011, Grasse *et al*. 2017). The first one focused on three pure SiO_2 materials: Diatomite ($\delta^{30}Si$= +1.26 ± 0.20 ‰; from hereon, all reproducibilities will be given as 2 standard deviations unless otherwise stated), IRMM-018 ($\delta^{30}Si$= -1.65 ± 0.22 ‰) and Big Batch ($\delta^{30}Si$= -10.48 ± 0.54 ‰; Reynolds *et al*. 2007). The Diatomite RM is still commonly included in analytical

sequences to check for accuracy and precision; however, the last two are less frequently utilised because they are either highly fractionated (Big Batch) or potentially inhomogeneous (IRMM-018, Reynolds *et al*. 2007). For a better matching between δ^{30}Si values of calibrators and samples, and to account for any microstructural effect, a second inter-laboratory comparison reported on a Southern Ocean sponge material as an additional RM for sponge spicule analyses (Hendry *et al*. 2011). A third inter-calibration study was motivated by the need to reliably compare the increasing number of Si isotope datasets of natural waters. Calibrators such as Diatomite (which is provided as a powdered, near-pure SiO_2 sample) cannot account for any biases introduced by the specific sample preparation and matrices involved when dealing with natural waters. These samples may contain Si with concentration below 20 µmol l^{-1}, which may require pre-concentrations steps or the processing of large amounts of sample, with potentially high salinity. With this in mind, Grasse *et al*. (2017) characterised two seawater samples (ALOHA 300, [Si]= 9 µmol l^{-1}, δ^{30}Si= +1.66 ± 0.13 ‰; ALOHA 1000, [Si]= 113 µmol l^{-1}, δ^{30}Si= +1.25 ± 0.06 ‰). The analysis of these "ALOHA" reference materials are now recommended when laboratories are reporting on seawater Si isotope data. In addition to this collection of RMs, there are more than a dozen silicate rock RMs that have enough extant published data to be suitable as calibrators for silicate rock analyses (e.g., Abraham *et al*. 2008, Hughes *et al*. 2011, Zambardi and Poitrasson 2011, Savage *et al*. 2014). Among these RMs, the Hawaiian basalt BHVO-2 (provided by the USGS) is the most commonly analysed. A valuable compilation of δ^{30}Si values suggests that the reference value for BHVO-2 is δ^{30}Si= -0.28 ± 0.03 ‰ (Savage *et al*. 2014) and more data are added continuously (see the GeoReM database).

Among the possible matrix effects on Si isotope measurements, the presence of anions such as sulfate (Van den Boorn *et al*. 2009) or dissolved organic carbon (DOC) (Hughes *et al*. 2011) has been reported to produce mass bias changes during MC-ICP-MS analysis. The issue remain debated as matrix effects induced by sulfate on Si isotopes were not subsequently confirmed (Georg *et al*. 2006, Zambardi and Poitrasson 2011, de Souza *et al*. 2012) and could potentially depend on plasma conditions of the MC-ICP-MS (Fietzke and Frische 2015, Yu *et al*. 2020). A recent study provides constraints on matrix anion threshold concentrations and the extent of resulting biases, but the role of instrument type and different sample introduction systems (wet

and dry plasma) has not been fully addressed (Oelze *et al*. 2016). However, as far as we are aware, there are no Si isotope data for RMs with an organic-rich matrix. Because such a matrix is prone to induce δ^{30}Si bias during MC-ICP-MS analysis, a lack of suitable RMs is an issue of major importance for the analysis of soil or plant material.

The aim of this paper is to provide the community with a set of easily available, well-characterised RMs containing organic material as part of the matrix for use as secondary RMs in Si isotope measurement. We propose four soil RMs (i.e., GBW-07401, GBW-07404, GBW-07407, TILL-1), representative of solid samples with a complex matrix with various Si-bearing phases (i.e., amorphous and/or crystalline silicate minerals, refractory minerals like iron oxy-hydroxides) and organic matter. In addition, the plant reference material ERM-CD281 (rye grass) was selected to represent the chemical composition of vegetation. It contains both organic matter and amorphous silica, which represents the form of Si generally accumulated in grass and then soils upon plant decay. This approach is an essential step in supporting δ^{30}Si data comparison among and within laboratories over time.

Materials and methods

Investigated materials

This study investigates four soil RMs GBW-07401, GBW-07404, GBW-07407, TILL-1 and one plant RM ERM-CD281. The GBW soils "set", developed by the Institute of Geophysical and Geochemical Exploration (IGGE) of the Chinese Academy of Geological Sciences (CAGS) is not commercially available any longer. Because of this, an aliquot (~ g) of the batches analysed in this study can be obtained upon request to Isabelle Basile-Doelsch at the Centre Européen de Recherche et d'Enseignement en Géosciences de l'Environnement, France (CEREGE). Reference material TILL-1 is provided by the CCRMP (Canadian Certified Reference Materials Project) and ERM-CD281 is provided by the EC-JRC (European Commission – Joint Research Center), and both are readily available to the community.

GBW-07401 is described as a dark brown podzolitic soil collected in a lead-zinc ore area, Heilongjiang, China; GBW-07404, as a limy-red soil obtained from Guangxi, China and GBW-07407, as a lateritic soil developed on basalt collected from Leizhou Peninsula, Guangdong, China (Wang *et al*. 2013). The reference material TILL-1 combines horizons B and C of a soil collected 25 km north-west of Lanark, Ontario, Canada (Lynch 1996). Among those soil RMs, SiO_2 content ranges from 32.67 to 62.60 % *m*/*m*, organic carbon (C_{org})content varies from 0.62 to 1.80 % *m*/*m* and sulfur content varies from 5 to 310 µg g^{-1} (more details in Table 1). The plant reference material ERM-CD281 is a rye grass, harvested in the United Kingdom in 1983, containing 0.13 % *m*/*m* Si (C_{org} unknown) and 34 µg g^{-1} S (Table 1).

Sample preparation and silicon isotope measurements

The reference materials were analysed for their δ^{29}Si and δ^{30}Si values in seven laboratories: University of Bristol Isotope Group, United Kingdom (BIG); CEREGE; Géosciences Environnement Toulouse, France (GET); German Research Centre for Geosciences, Germany (GFZ); Institut Français de Recherche pour l'Exploitation de la Mer, France (IFREMER); St Andrews Isotope Geochemistry, University of St Andrews, United Kingdom (STAiG); and Water Quality Centre – Trent University, Canada (WQC). The RMs, provided as homogeneous powders by suppliers, were split and spread among the different laboratories via mail. Laboratories each received an aliquot of about 1 g of GBW soil RMs, 0.2 g of TILL-1 and 3 g of ERM-CD281. Each laboratory conducted sample preparation and Si isotope measurements using their own protocols as detailed in Table 2. Sample preparation protocols of all laboratories are adapted from Georg *et al*. (2006) and hence are similar and consist of an alkaline fusion step followed by purification on a cation exchange resin. In the following, we highlight the differences between the sample preparation and measurement protocols. More details on the procedures used in each participating laboratory are given in previous publications or in the online supporting information Appendix S1. For BIG see Hatton *et al*. (2019); for CEREGE see Appendix S1; for GET see Zambardi and Poitrasson (2011); for GFZ see Schuessler and von Blanckenburg (2014) and Oelze *et al*. (2016); for IFREMER see Bayon *et al*. (2018); for STAiG see Savage and Moynier (2013); for WQC see Georg *et al*. (2006).

One major difference between protocols relates to the use of calcination to mineralise organic matter. CEREGE, GET and WQC calcinated the samples before fusion while BIG, GFZ and IFREMER did not; STAiG processed replicates both with and without calcination (see Appendix S1 for detailed calcination procedures). All laboratories performed NaOH fusion in silver crucibles except for IFREMER who used NaOH and Na_2O_2 in glassy carbon crucibles (Bayon *et al*. 2018). Finally, in order to purify the samples, all laboratories used column chromatography with cation exchange resin (either AG50W-X12 or AG50W-X8, see Table 2) based on the procedure developed by Georg *et al*. (2006). After alkali fusion, samples are normally taken up in a weakly acidic solution; many laboratories perform a measurement of solution Si concentration here (prior to Si purification), firstly to check for quantitative yield from the fusion step, and also to calculate the required amount of solution for column chemistry.

After column chemistry, the purified Si solutions were analysed by ICP-OES, (MC-)ICP-MS or by spectrophotometer using the molybdenum blue colorimetric method to (i) verify quantitative Si column recovery (i.e., complete recovery within analytical reproducibilities of the concentration measurements of 100 ± 5%) and (ii) check the purity of the Si sample solutions, with a particular focus on confirming the lack of magnesium (Mg) within the sample in the laboratories using Mg doping. Purity was better than 95% for Si, except for the plant ERM CD-281, where elevated levels of phosphorous and sulfur (mass ratios PO_4/Si up to 5 and SO_4/Si up to 6), respectively were still present. Complete removal of these anions was achieved neither by high temperature volatilisation during NaOH fusion at 750 °C for 10 min (without prior calcination; GFZ) or calcination (CEREGE, no SO_4 data), or by the Si column chemistry. However, as discussed below, all impurities were still within the tolerance limits found to not cause any bias in Si isotope measurements using the MC-ICP-MS setup (instrument, sample introduction system, analyte matrix, Mg doping, etc.) used by the participating laboratories in this study.

Silicon isotope measurements were performed by MC-ICP-MS, either Neptune Plus MC-ICP-MS or Neptune MC-ICP-MS (both from Thermo Fisher Scientific, Germany) (Table 2). The analyses were performed in medium resolution ($M/\Delta M$ ~ 4500, 5 and 95% peak side definition, see Weyer and Schwieters 2003; except for GET which utilised high resolution ($M/\Delta M$ ~ 7–10000)) using

between 0.5–3.6 µg Si per analysis, which resulted in a 3–20 V ion beam on ^{28}Si. Four laboratories carried out analyses in 'wet plasma mode', three in 'semi-dry plasma mode' using a desolvating nebuliser system (ESI Apex-HF, ESI Apex Q). The main advantages of a desolvation unit are to reduce polyatomic interferences from oxygen, nitrogen, carbon and hydrogen, and to improve sensitivity. However, use of a desolvation unit increases matrix effects and results in a less stable signal. Subtraction of the blank signal (measured on the pure acid matrix solution) from all sample Si intensities was performed before subsequent data processing by all laboratories (BIG, GFZ, CEREGE, GET, STAiG). For all laboratories, full procedural blank Si intensities did not exceed 1% of the sample Si signal (Table 2).

All measurements were performed using the calibrator-sample-bracketing technique using NBS 28 (also named NIST SRM 8546) as the bracketing calibrator, except for IFREMER where an in-house calibrator previously calibrated against the NBS 28 was used. With the exception of STAiG and WQC laboratories, the purified Si solutions were also doped with Mg (Si:Mg ratio of 1 to 3, depending on the laboratories; Table 2) prior to mass spectrometric analysis for an additional online mass bias drift correction using an exponential mass bias equation (Cardinal *et al*. 2003, Engström *et al*. 2006, Zambardi and Poitrasson 2011, Oelze *et al*. 2016), (Table 2). When Mg-doping was utilised, Mg isotopes were analysed along Si isotopes using dynamic mode (magnet jump alternating between Si and Mg isotopes) for each sample doped with Mg. Magnesium doping is also useful to eliminate variations due to sample matrix effects or insufficiently stable laboratory temperature (Cardinal *et al*. 2003, Engström *et al*. 2006, Zambardi and Poitrasson 2011, Oelze *et al*. 2016). Additionally, BIG samples were doped with 50 µl 0.01 mol l^{-1} sulfuric acid per ml of sample to reduce anionic matrix effects. Silicon isotope compositions are reported (‰) relative to the NBS 28 in the delta notation as δ^{30}Si and δ^{29}Si:

$$\delta^{30,\,29}\mathrm{Si} = (R_{\mathrm{sample}}/R_{\mathrm{NBS\ 28}}) - 1 \qquad (1)$$

where R is the ratio ^{30}Si/^{28}Si or ^{29}Si/^{28}Si in a sample, and $R_{\mathrm{NBS\ 28}}$ the mean value for reference material NBS 28 calculated using the mean of the measured Si isotope ratio immediately measured before and after the unknown sample (i.e., calibrator-sample bracketing).

The well-characterised Diatomite and/or BHVO-2 RMs, for which large datasets are available in the literature, were measured routinely for quality control as unknown samples during the runs by all laboratories to check for accuracy and precision. These data are provided in Table 2, and are in good agreement with the published values compiled in Table S1 (i.e., mean δ^{30}Si = -0.28 ± 0.08 ‰ (*U*, *k* = 2, *N* = 61 where *N* is the number of data published)).

At least three aliquots of each RM used in this study were processed through the whole sample preparation at each laboratory, hereafter referred to as full procedure replicates, except for GET (*N* = 1), WQC (*N* = 1) and an additional uncalcinated aliquot of GBW-07401 and GBW-07407 processed by STAiG. Each full procedure replicate was then analysed between three and fourteen times either on different days or on the same day but not consecutively depending on laboratories (see Table 2 for details). Each mass spectrometric analysis consisted of between twenty to thirty-six signal integrations of 4 to 8.4 s, which is a total 80 to 210 s of Si signal acquisition per analysis. For each laboratory, replicate measurements carried out for each RM full procedure replicate were averaged using the arithmetic mean and its associated 2 standard deviation (2*s*; data are reported in Table S2).

Results and discussion

Data quality of participating laboratories

An essential measurement control is given by the three-isotope plot (Figure 1). All data (from the RMs full procedural replicates reported by each laboratory) fall on a straight line with a slope of about δ^{29}Si ~ 0.5103 × δ^{30}Si (r^2 > 99%). The linear correlation encompasses the theoretical slopes calculated for both equilibrium (0.5178) and kinetic (0.5092) mass-dependent fractionation processes (Engström *et al*. 2008), suggesting no major influence of isobaric interferences or matrix effects. In addition, the δ^{30}Si and δ^{29}Si values of the Diatomite and BHVO-2 RMs measured by all laboratories agree well with compiled values (Reynolds *et al*. 2007, Savage *et al*. 2014, our compilation in Table S1). The absolute differences between published values and those produced

by participating laboratories are smaller than 0.06 ‰ and 0.03 ‰ for δ^{30}Si and δ^{29}Si, respectively, which are within the 2*s* reported by each laboratory (Table 2).

WQC reported δ^{30}Si calculated from measured δ^{29}Si assuming an equilibrium mass-dependent fractionation. Comparing WQC δ^{30}Si results with values reported by other laboratories (Figure 2) shows no notable difference between their calculated δ^{30}Si and other laboratories measured δ^{30}Si, within their respective 2*s*. This approach is therefore valid for the set of RMs analysed in this study. However, this approach should be used with caution since it does not allow a data quality check for mass-dependent fractionation using the three-isotope plot (Figure 1).

Individual results of soil reference materials

The δ^{30}Si and δ^{29}Si values obtained for each full procedural replicate of each RM by participating laboratories are illustrated in Figure 2 and provided in Table S2. The Si isotope composition of the five RMs reported are indistinguishable within 2*s*, both between the full procedural replicates for a given laboratory, and also between laboratories. The δ^{30}Si data range between -0.30 ‰ < δ^{30}Si < -0.20 ‰ for GBW-07401; -0.90 ‰ < δ^{30}Si < -0.67 ‰ for GBW-07404; -2.05 ‰ < δ^{30}Si < -1.71 ‰ for GBW-07407; -0.21 ‰ < δ^{30}Si < -0.12 ‰ for TILL-1. This range of δ^{30}Si values spans the typical δ^{30}Si spectrum of soil materials ranging from -2.7 ‰ to +0.1 ‰ (Poitrasson 2017). The most negative Si isotope compositions are measured in the RMs with the lowest SiO_2/Al_2O_3 mass ratio (GBW-07407), i.e., the soil that has undergone the most desilicification (Figure 3). This is consistent with the general weathering trend, wherein the Si isotopic composition of secondary clay minerals formed during chemical weathering is lower than that of the primary silicate material (e.g., Opfergelt *et al*. 2010, Georg *et al*. 2009, Savage *et al*. 2013). Furthermore, the formation of more desilicified 1:1 clays is accompanied by a larger (negative) Si isotopic fractionation than the formation 2:1 clays (Georg *et al*. 2009, Opfergelt *et al*. 2012).

Individual results for plant reference material ERM-CD281

Of the laboratories involved in this study, two did not analyse the ERM-CD281 (rye grass) because they had not previously processed highly organic-rich material (i.e., plant matter) and methodological development was beyond the scope of this study. The δ^{30}Si and δ^{29}Si obtained

for the plant RM full procedure replicates by each laboratory are illustrated in Figure 2 and provided in Table S2. The Si isotope compositions reported are indistinguishable within 2*s* both between the full procedural replicates for a given laboratory and between laboratories. The δ^{30}Si data range between -0.36 ‰ < δ^{30}Si < -0.26 ‰. In addition to the data acquired during this study, another published result for ERM-CD281 is available (δ^{30}Si = -0.28 ± 0.08 ‰, 2*s*, *n* = 3, Frick *et al*. 2020). These published analyses were performed at GFZ using the same protocol in the same laboratory as reported for GFZ in this study. The Si isotope values for ERM-CD281 fall within the large range of δ^{30}Si values reported in the literature for biogenic silica in plants (-2.3 to +6.1 ‰, Opfergelt and Delmelle 2012). The range of Si isotope compositions is large because the δ^{30}Si values of biogenic silica in plants depend on several factors such as soil parent material lithology, soil weathering degree and on complex isotope fractionation processes during Si uptake and deposition (Opfergelt *et al*. 2010).

Influence of sulfur and DOC contents

The importance of chemical purification in removing so-called matrix effects has already been described for several isotopes systems measured by MC-ICP-MS (see for example Galy *et al*. 2001, for Mg isotopes). For Si isotopes, significant effects induced by the presence of sulfur in rock samples were first reported by Van den Boorn *et al*. (2009), i.e., a Si isotope bias of up to 1.4 ‰ for a SO_4/Si mass ratio higher than 0.02. Subsequent studies have discussed the possibility of sulfur-induced bias on Si isotope measurements (Hughes *et al*. 2011, Zambardi and Poitrasson 2011, Chemtob *et al*. 2015), and highlighted the potential for several parameters to influence the magnitude of the bias, notably in the dry plasma mode (Oelze *et al*. 2016). Thus, care must be taken when comparing studies as drawing conclusions is not straightforward. In particular, comparing sulfur-induced bias between S-doped solutions and S-rich rocks is likely irrelevant. However, in this study, sulfur-induced matrix effects are less likely to be significant, because the 720 °C fusion step of solid samples used by all laboratories will at least partially remove the sulfur, with full removal achieved by heating at 1350 °C (Van den Boorn *et al*. 2009). Despite different analytical settings, this can partly explain the large decrease from +1.4 to +0.3 ‰ (SO_4/Si mass ratio ~ 0.3) between Van den Boorn *et al*. (2009) and Hughes *et al*. (2011) datasets as well as the absence of Si isotope bias measured on rock samples with SO_4/Si mass ratios ≤ 0.14

by Zambardi and Poitrasson (2011). To allow comparison between studies, it would be useful to provide SO_4/Si ratios of the Si analyte solutions in addition to the usual initial sample SO_4/Si ratios before processing. Restricting comparison to S-doped pure Si solutions (usually doped NBS 28), it appears that several parameters may reduce the isotopic bias. Van den Boorn *et al*. (2009) noticed that 0.1 mol l^{-1} HCl matrix reduces the bias by a factor about 1.5 compared with a HNO_3 matrix. Also, Chemtob *et al*. (2015) noticed no significant bias due to sulfur for SO_4/Si mass ratios <1 with a 0.002% HF and 2% HNO_3 matrix despite very similar analytical parameters (i.e., the use of a Neptune, a CETAC desolvator and no Mg doping). It appears that the overall sample aliquot matrix plays a role in the magnitude of the S-induced bias in addition to subtle differences in instrumental set-up. Similarly, Georg *et al*. (2006) noticed no deviation from expected values for SO_4/Si mass ratio up to 48 using a Nu instrument, a CETAC desolvator in a 0.1 mol l^{-1} HCl matrix without Mg doping. Similarly, Zambardi and Poitrasson (2011) and Oelze *et al* (2016) investigated the effect with Mg doping. For SO_4/Si ratios < 1, the Mg doping had no effect on the magnitude of the S-induced bias (Zambardi and Poitrasson 2011, Oelze *et al*. 2016). Moreover, Oelze *et al* (2016) found that the addition of Mg to the Si analyte solution resulted in higher tolerance to impurities during MC-ICP-MS analyses when an Apex desolvator without a membrane was used. Remaining anionic impurities (PO_4^{3-}, SO_4^{2-} and NO_3^-) had no effect on the Si isotope mass bias (with accuracy within ± 0.14 ‰) if the mass ratio of those anions to Si is lower than 6 (Oelze *et al*. 2016). To overcome S-induced bias, different techniques were suggested: removal of sulfur by heating the samples up to 1350 °C (Van den Boorn *et al*. 2009) or doping both samples and bracketing calibrator with significant amounts of sulfuric acid to overwhelm any variation in the sample (Hughes *et al*. 2011).

In this study, no S-induced bias on Si isotopes measurements is expected for soil RMs as SO_4/Si mass ratios are below 0.01 (SO_4/Si mass ratio ~ 0.003 for GBW-07401; 0.002 for GBW-07404; 0.005 for GBW-07407 and 0.002 for TILL-1). In contrast, the plant RM ERM-CD281 has a SO_4/Si mass ratio about 7.8 that could potentially be problematic for Si isotope measurements. This was verified in Si analyte solutions where elevated levels of phosphorous and sulfur (mass ratios PO_4/Si up to 5 and SO_4/Si up to 6), respectively, were still present after NaOH fusion (with or without prior calcination) and Si column purification. Complete removal of these anions was

achieved neither by high temperature volatilisation nor by the Si column chemistry. However, all impurities were still within the limits required to avoid any bias for all different analytical configurations used by different laboratories (prior calcination or not, wet plasma or Apex desolvation, Mg doping or no Mg doping, HCl or HNO_3 matrix). This is consistent with the study of Oelze *et al*. (2016) where no effect on the Si isotope mass bias was observed when the mass ratio of anions to Si was lower than 6 with an Mg correction (1 without an Mg correction). The Si isotope results of ERM CD-281 measured by laboratories using a regular spray chamber (wet plasma) agree well with those measured using an Apex sample introduction system. Similarly, the prior calcination of the sample has a limited effect (Figure 2) and does not seem mandatory for SO_4 removal in such samples. In all cases, the chemical preparation and analytical settings seem to be robust enough to avoid matrix effects caused by residual impurities in the sample during Si isotope measurements.

Hughes *et al*. (2011) also showed that measurable concentrations of dissolved organic carbon (DOC) in freshwater samples can affect their Si isotopic determination. Given the large spectrum of naturally occurring DOC forms, DOC-induced bias is suspected to vary from one DOC form to another even before considering combined effects. This would make correcting for the presence of DOC in samples unworkable, due to the near-impossibility of matching the matrix in the bracketing calibrators. Therefore, removal of organic matter during sample preparation seems to be the best option to ensure reliable analysis of organic carbon-rich samples.

The variability of the SiO_2 and organic carbon contents of the soils RMs used in this study allow for evaluation of the influence of varying matrix to analyte ratios with or without calcination steps. When comparing the results with or without organic matter mineralisation, no notable offset is observed, regardless of the considered RM (Figure 2). In addition, STAiG laboratory calcinated their RMs but also processed one aliquot each of GBW-07401 and GBW-07407 without calcination (Figure 2). The results for both calcinated and uncalcinated aliquots of these two RMs are identical within 2*s* (Figure 2 and Table S2). In addition, at GFZ the removal of organic carbon by the NaOH fusion method (750 °C, 10 min) – without prior calcination – was investigated. Effective organic carbon removal was found for all soil and plant samples processed

at GFZ during this study using semi-quantitative ICP-OES analyses (carbon 193.027 nm emission line) by evaluation of C remaining in the post-fusion and purified Si solutions prior to Si isotope measurements. All solutions showed C-counts indistinguishable from pure acid used for dilution for the analyses, whereas significant C intensities were recorded in sample aliquots that were not treated by alkali fusion and subsequent Si column purification. It thus seems that the presence of organic carbon has no impact on the accuracy or reproducibility of Si isotopes measurements if the high temperature alkaline fusion digestion is used (with or without prior calcination) as the residual organic matter does not induce Si isotopic bias. Several factors could explain this. The amount of organic matter in uncalcinated aliquots was insufficient to induce any bias. Indeed, C_{org}/Si mass ratios of soil RMs were below 0.1 while Hughes *et al*. (2011) observed a shift in freshwater samples from DOC/Si > 0.2. However, the Si isotope measurement of the high C_{org}/Si plant RM ERM-CD281 analysed at IFREMER and GFZ – without prior calcination step – are not affected. In this case, it could be that the organic carbon in this sample is not refractory and is oxidised during the high-temperature fusion step as suggested by C analyses at GFZ. Finally, it is also possible that the DOC form present in soils or plants does not induce bias, at least not on the Thermo Neptune-family of MC-ICP-MS instruments. More tests would be required to determine the critical DOC/Si ratio and if it is DOC-form sensitive.

Assigning δ^{30}Si and δ^{29}Si to the reference materials analysed in this study

Results from all seven laboratories are in excellent agreement for all RMs (Figure2), despite the use of different sample preparations (calcination versus no calcination; NaOH fusion versus NaOH and Na_2O_2 fusion) and different analytical settings (Mg doping vs. no doping, wet plasma sample introduction vs. semi-dry plasma; see Table 2). Therefore, the results reported by the laboratories for each RM full procedural replicate (with the exception of the δ^{30}Si reported by WQC) were weighted and combined together to calculate means and their associated combined uncertainties (U, k = 2). Final isotopic characterisation of the five RMs analysed here are given in Table 3. Following the EURACHEM/CITAC Guide CG4, the combined uncertainties were calculated by error propagation, assuming independent variables, of the standard deviations obtained on full procedural replicates for each RM, including the standard deviation of the means of full procedure replicates for each RM. The combined uncertainties were multiplied by a coverage

factor of k = 2 to obtain the expanded uncertainties for each RM. The uncertainties (U, k = 2) range from 0.04 ‰ to 0.12 ‰ for δ^{29}Si and from 0.06 ‰ to 0.17 ‰ for the δ^{30}Si. The larger magnitude of U for δ^{30}Si compared with those for δ^{29}Si correspond with the lower natural abundance of ^{30}Si compared with ^{29}Si and the concomitant deterioration in counting statistics of the detectors. In addition, the uncertainties of these results (Table 3) are comparable to the standard deviation obtained on multiple measurements of the RMs Diatomite and BHVO-2 (Table 2) used by the laboratories to check for accuracy. Overall, the homogeneity of the reference materials is valid at the scale of the minimum test portion mass used in this study, i.e., > 3 mg for the soil RMs, and at least 50 mg for rye grass ERM CD281. The soil RMs GBW-07401, GBW-07404, GBW-07407 and TILL-1 offer a wide range of δ^{29}Si and δ^{30}Si values comparable with and therefore useful for future Si isotope environmental studies. The uncertainties obtained in this inter-laboratory comparison are more than one order of magnitude lower than the range of δ^{29}Si and δ^{30}Si measured in natural samples: -5.7 to +6.1 ‰ (Opfergelt and Delmelle 2012) and are therefore sufficient to allow the robust interpretation of small variations in the δ^{29}Si and δ^{30}Si.

Conclusions

In this study, the δ^{29}Si and δ^{30} Si values of four soil and one plant reference material were determined and compared between laboratories. Different sample preparation procedures and analytical settings provide consistent results for both δ^{29}Si and δ^{30}Si values for all RMs. Therefore, all protocols used by the participating laboratories for Si isotope analysis provide comparable results. Also, no notable isotopic bias was observed between calcinated and uncalcinated RMs with different C_{org}/Si ratios. However, caution still stands for analyses of organic carbon-rich samples with a C_{org}/Si ratio above the studied RMs, where biases in δ^{30}Si measurements could potentially occur. This is particularly the case when sample preparation does not involve calcination, leading to potential matrix effects during MC-ICP-MS analyses that could be DOC-form dependent. The data for soil and plant reference materials from this study can be reliably used by other laboratories for routine quality control of Si isotope ratio measurements during environmental and geochemical studies. Moreover, the wide range of

δ^{29}Si and δ^{30}Si covered by these soil RMs provided here allows analysts to select the RMs that are best suited for their study.

Acknowledgements

At CEREGE, this project was initiated by an EIL funding from the Société Française des Isotopes Stables (SFIS) and also supported by the Agence Nationale pour la Recherche (ANR, France) through the project EQUIPEX ASTER-CEREGE and the project BIOSiSOL (ANR-14-CE01-002). C.D. is funded by the "Fonds National de la Recherche Scientifique" (Belgium). SF and the Si isotope measurements at STAiG were supported by NERC grant NE/R002134/1 to PS; PS would also like to cite the support of a Carnegie Trust Research Incentive Grant, which helped the setup of various isotope techniques in the St Andrews Isotope Geochemistry (STAiG) laboratories. F. von Blanckenburg and the Helmholtz Association are thanked for infrastructure support at GFZ. At the University of Bristol, C.D. Coath is thanked for laboratory support and the European Research Council is acknowledged for funding (ICY-LAB, grant agreement 678371). Hélène Mariot is thanked for her careful maintenance of the CEREGE clean lab. Manuel Henry and Jérôme Chmeleff are thanked for maintaining the GET clean lab and MC-ICP-MS facilities in good working order. J. Schlegel and J. Buhk are acknowledged for laboratory support at GFZ. The authors declare that there is no conflict of interest.

Data availability Statement

The authors confirm that the data supporting the findings of this study are available within the article and its online supporting information. Detailed datasets are available from the corresponding author upon reasonable request.

References

Abraham K., Opfergelt S., Fripiat F., Cavagna A.J., de Jong J.T.M., Foley S.F., André L. and Cardinal D. (2008)

$\delta^{30}Si$ and $\delta^{29}Si$ determinations on USGS BHVO-1 and BHVO-2 reference materials with a new configuration on a Nu plasma multi-collector ICP-MS. **Geostandards and Geoanalytical Research, 32**, 193–202.

Barnes I.L., Moore L.J., Machlan L.A., Murphy T.J. and Shields W.R. (1975)
Absolute isotopic abundance ratios and the atomic weight of a reference sample of silicon. **Journal of Research of the National Bureau of Standards. Section A, 79A**, 727–735.

Basile-Doelsch I. (2006)
Si stable isotopes in the Earth's surface: A review. **Journal of Geochemical Exploration, 88**, 252–256.

Bayon G., Delvigne C., Ponzevera E., Borges A.V., Darchambeau F., De Deckker P., Lambert T., Monin L., Toucanne S. and André L. (2018)
The silicon isotopic composition of fine-grained river sediments and its relation to climate and lithology. **Geochimica et Cosmochimica Acta, 229**, 147–161.

Berner R.A., Lasaga A.C. and Garrels R.M. (1983)
The carbonate-silicate geochemical cycle and its effect on atmospheric carbon dioxide over the past 100 million years. **American Journal of Science, 283**, 641–683.

Cardinal D., Alleman L.Y., de Jeong J., Ziegler K. and André L. (2003)
Isotopic composition of silicon measured by multicollector plasma source-mass spectrometry in dry plasma mode. **Journal Analytical Atomic Spectrometry, 18**, 213–218.

Chemtob M., Rossman G.R., Young E.D., Ziegler K., Moynier F., Eiler J.M. and Hurowitz J.A. (2015)
Silicon isotope systematics of acidic weathering of fresh basalts, Kilauea Volcano, Hawai'i. **Geochimica et Cosmochimica Acta, 169**, 63–81.

Conley D.J. (2002)

Terrestrial ecosystems and the global biogeochemical silica cycle. **Global Biogeochemical Cycles, 16**, 1121, doi:10.1029/2002 gb001894

de Souza G.F., Reynolds B.C., Rickli J., Frank M., Saito M.A., Gerringa L.J.A. and Bourdon B. (2012)

Southern Ocean control of silicon stable isotope distribution in the deep Atlantic Ocean. **Global Biogeochemical Cycles, 26**, GB2035, doi:10.1029/2011GB004141

De Bièvre P. and Taylor P.D.P. (1993)

Table of the isotopic compositions of the elements. **International Journal of Mass Spectrometry and Ion Processes, 123**, 149–166.

Engström E., Rodushkin I., Baxter D.C. and Öhlander B. (2006)

Chromatographic purification for the determination of dissolved silicon isotopic compositions in natural waters by high-resolution multicollector inductively coupled plasma-mass spectrometry. **Analytical Chemistry, 78**, 250–257.

Engström E., Rodushkin I., Öhlander B., Ingri J. and Baxter D.C. (2008)

Silicon isotopic composition of boreal forest vegetation in northern Sweden. **Chemical Geology, 257**, 247–256.

Engström E., Rodushkin I., Ingri J., Baxter D.C., Ecke F., Osterlund H. and Ohlander B. (2010)

Temporal isotopic variations of dissolved silicon in a pristine boreal river. **Chemical Geology, 271**, 142–152.

Fietzke J. and Frische M. (2015)

Experimental evaluation of elemental behavior during LA-ICPMS: influences of plasma conditions and limits of plasma robustness. **Journal of Analytical Atomic Spectrometry, 31**, 234–244.

Frick D.A., Remus R., Sommer M., Augustin J. and von Blanckenburg F. (2020)
Silicon isotope fractionation and uptake dynamics of three crop plants: Laboratory studies with transient silicon concentrations. **Biogeosciences Discussions**, https://doi.org/10.5194/bg-2020-66, in review.

Galy A., Belshaw N.S., Halicz L. and O'Nions R.K. (2001)
High-precision measurement of magnesium isotopes by multiple collector inductively coupled plasma-mass spectrometry. **International Journal of Mass Spectrometry, 208**, 89–98.

Georg R.B., Reynolds B.C., Frank M. and Halliday A.N. (2006)
New sample preparation techniques for the determination of Si isotopic compositions using MC-ICP-MS. **Chemical Geology, 235**, 95–104.

Georg R.B., West A.J., Basu A.R. and Halliday A.N. (2009)
Silicon fluxes and isotope composition of direct groundwater discharge into the Bay of Bengal and the effect on the global ocean silicon isotope budget. **Earth and Planetary Science Letters, 283**, 67–74.

Grasse P., Brzezinski M.A., Cardinal D., de Souza G.F., Andersson P., Closset I., Cao Z., Dai M., Ehlert C., Estrade N., François R., Frank M., Jiang G., Jones J.L., Kooijman E., Liu Q., Lu D., Pahnke K., Ponzevera E., Schmitt M., Sun X., Sutton J.N., Thil F., Weis D., Wetzel F., Zhang A., Zhang J. and Zhang Z. (2017)
GEOTRACES inter-calibration of the stable silicon isotope composition of dissolved silicic acid in seawater. **Journal Analytical Atomic Spectrometry, 32**, 562–578.

Hatton J.E., Hendry K.R., Hawkings J.R., Wadham J.L., Kohler T.J., Stibal M., Beaton A.D., Bagshaw E.A. and Telling J. (2019)
Investigation of subglacial weathering under the Greenland Ice Sheet using silicon isotopes. **Geochimica et Cosmochimica Acta, 247**, 191–206.

Hendry K., Leng M., Robinson L., Sloane H., Blusztjan J., Rickaby R., Georg R.B., Halliday, A. (2011)

Silicon isotopes in Antarctic sponges: An interlaboratory comparison. **Antarctic Science, 23**, 34–42.

Hughes H.J., Delvigne C., Korntheuer M., de Jong J., André L. and Cardinal D. (2011)

Controlling the mass bias introduced by anionic and organic matrices in silicon isotopic measurements by MC-ICP-MS. **Journal Analytical Atomic Spectrometry, 26**, 1892–1896.

Hughes H.J., Sondag F., Santos R.V., André L. and Cardinal D. (2013)

The riverine silicon isotope composition of the Amazon Basin. **Geochimica et Cosmochimica Acta, 121**, 637–651.

Jochum K.P., Nohl U., Herwig K., Lammel E., Stoll B. and Hofmann A.W. (2005)

GeoReM: A new geochemical database for reference materials and isotopic standards. **Geostandards and Geoanalytical Research, 29**, 333–338.

Lynch J. (1996)

Provisional elemental values for four new geochemical soil and till reference materials, TILL-1, TILL-2, TILL-3 and TILL-4. **Geostandards Newsletter, 20**, 277–287.

Mangalaa K.R., Cardinal D., Brajard J., Rao D.B., Sarma N.S., Djouraev I., Chiranjeevulu G., Murty K.N. and Sarma V.V.S.S. (2017)

Silicon cycle in Indian estuaries and its control by biogeochemical and anthropogenic processes. **Continental Shelf Research, 148**, 64–88.

Nelson D.M., Tréguer P., Brzezinski M.A., Leynaert A. and Quéguiner B. (1995)

Production and dissolution of biogenic silica in the ocean: Revised global estimates, comparison with regional data and relationship to biogenic sedimentation. **Global Biogeochemical Cycles, 9**, 359–372.

Oelze M., Schuessler J.A. and von Blanckenburg F. (2016)
Mass bias stabilization by Mg doping for Si stable isotope analysis by MC-ICP-MS. **Journal of Analytical Atomic Spectrometry, 31**, 2094–2100.

Opfergelt S., Cardinal D., André L., Delvigne C., Bremond L. and Delvaux B. (2010)
Variations of $\delta^{30}Si$ and Ge/Si with weathering and biogenic input in tropical basaltic ash soils under monoculture. **Geochimica et Cosmochimica Acta, 74**, 225–240.

Opfergelt S. and Delmelle P. (2012)
Silicon isotopes and continental weathering processes: Assessing controls on Si transfer to the ocean. **Comptes Rendus Geoscience, 344**, 723–738.

Poitrasson F. (2017)
Silicon isotope geochemistry. **Reviews in Mineralogy and Geochemistry, 82**, 289–344.

Ragueneau O., Schultes S., Bidle K., Claquin P. and Moriceau B. (2006)
Si and C interactions in the world ocean: Importance of ecological processes and implications for the role of diatoms in the biological pump. **Global Biogeochemical Cycles, 20**, GB4S02.

Reynolds B.C., Aggarwal J., André L., Baxter D., Beucher C., Brzezinski M.A., Engström E., Georg R.B., Land M., Leng M.J., Opfergelt S., Rodushkin I., Sloane H.S., van den Boorn S.H.J.M., Vroon P.Z. and Cardinal D. (2007)
An inter-laboratory comparison of Si isotope reference materials. **Journal of Analytical Atomic Spectrometry, 22**, 561–568.

Savage P.S., Georg R.B., Williams H.M. and Halliday A.N. (2013)
The silicon isotope composition of the upper continental crust. **Geochimica et Cosmochimica Acta, 109**, 384–399.

Savage P.S., Armytage R.M.G., Georg R.B. and Halliday A.N. (2014)
High temperature silicon isotope geochemistry, **Lithos, 190**, 500–519.

Savage P.S. and Moynier F. (2013)
Silicon isotopic variation in enstatite meteorites: Clues to their origin and Earth forming material. **Earth and Planetary Science Letters, 361**, 487–496.

Schuessler J.A. and von Blanckenburg F. (2014)
Testing the limits of micro-scale analyses of Si stable isotopes by femtosecond laser ablation multicollector inductively coupled plasma-mass spectrometry with application to rock weathering. **Spectrochimica Acta Part B, 98**, 1–18.

Street-Perrott F.A. and Barker P.A. (2008)
Biogenic silica: A neglected component of the coupled global continental biogeochemical cycles of carbon and silicon. **Earth Surface Processes and Landforms, 33**, 1436–1457.

Struyf E. and Conley D.J. (2012)
Emerging understanding of the ecosystem silica filter. **Biogeochemistry, 107**, 9–18.

van den Boorn S.H.J.M., Vroon P.Z. and Bergen M.J. (2009)
Sulfur-induced offsets in MC-ICP-MS silicon-isotope measurements. **Journal of Analytical Atomic Spectrometry, 24**, 1111–1114.

Vandevenne F.I., Delvaux C., Hughes H.J., André L., Ronchi B., Clymans W., Barão L., Govers G., Meire P., Struyf E. and Cornelis J.T. (2015)
Landscape cultivation alters δ^{30}Si signature in terrestrial ecosystems. **Scientific Reports, 5**, 7732.

Weyer S. and Schwieters J. (2003)
High precision Fe isotope measurements with mass resolution MC-ICP-MS. **International Journal of Mass Spectrometry, 226**, 355–368.

Yu Y., Siebert C., Fietzke J., Goepfert T., Hathorne E., Cao Z. and Frank M. (2020)
The impact of MC-ICP-MS plasma conditions on the accuracy and precision of stable isotope measurements evaluated for barium isotopes. **Chemical Geology, 549**, 110697.

Zambardi T. and Poitrasson F. (2011)
Precise determination of silicon isotopes in silicate rock reference materials by MC-ICP-MS. **Geostandards and Geoanalytical Research, 35**, 89–99.

Supporting information

The following supporting information may be found in the online version of this article:

Appendix S1. Calcination procedures; Sample preparation and Si isotope ratio measurements at CEREGE.

Table S1. Compilation of published BHVO-2 $\delta^{30}Si_{NBS\ 28}$ estimates.

Table S2. Means of analytical replicates of $\delta^{30}Si_{NBS\ 28}$ and $\delta^{29}Si_{NBS\ 28}$, and associated 2*s*, number of analyses per full replicate preparation for each reference material.

This material is available from: http://onlinelibrary.wiley.com/doi/10.1111/ggr.00000/abstract
(This link will take you to the article abstract).

Figure captions

Figure 1. Three-isotope plot of δ^{29}Si and δ^{30}Si of the data for full procedural replicates of each reference material from each laboratory (see Table S2). Range bars are the 2*s* calculated from replicate analyses for each full procedure replicate. The mass-dependent equilibrium fractionation line (slope 0.5178 – solid line) and kinetic fractionation line (slope 0.5092 – dotted line) are shown (Engström *et al*. 2008).

Figure 2. δ^{30}Si results measured by each laboratory for each reference material (see Table 2 for the correspondence between laboratory number and laboratory name). Each data point is the arithmetic mean ± 2 standard deviations of at least three replicate analyses for each reference material full procedural replicate. The figure also shows whether the samples were calcinated (C) or not (NC) to remove organic matter before alkaline fusion as well as whether the Si fractions were doped (D) with Mg prior to mass spectrometric analyses or not (ND). The black star on the δ^{30}Si of WQC shows that this value was not measured but calculated from measured δ^{29}Si assuming mass-dependent fractionation. The vertical envelope between the dotted lines shows the array defined by the expanded uncertainty (*U*, *k* = 2) around the arithmetic mean of the full procedure replicates for each reference material.

Figure 3. Plot of $\delta^{30}Si_{NBS\ 28}$ against SiO_2/Al_2O_3 mass ratio in soil reference materials, showing the predicted behaviour of Si isotopes due to increased chemical weathering of a sample; specifically, neoformation of clay minerals preferentially enriches the secondary minerals in the lower atomic number ('lighter') Si isotopes (Opfergelt and Delmelle 2012).

Table 1.									
SiO_2, Al_2O_3, C, S contents and SiO_2/Al_2O_3 mass ratios in investigated reference materials									
	SiO_2	±	Al_2O_3	±	SiO_2/Al_2O_3	C	±	S	±
	(% *m/m*)		(% *m/m*)		mass ratio	(% *m/m*)		(µg g^{-1})	
GBW-07401	62.60	0.14	14.18	0.14	4.41	1.80	0.16	310	
GBW-07404	50.95	0.14	23.45	0.19	2.17	0.62	0.08	180	36
GBW-07407	32.67	0.18	29.26	0.34	1.12	0.64	0.07	250	36
TILL-1	60.9		13.7		4.45	unknown		< 5	
ERM-CD281	0.28		unknown		unknown	unknown		unknown	

Table 2.

Detailed overview of chemical preparation and analytical techniques used by each laboratory

Laboratory	BIG	CEREGE	GET	GFZ
Laboratory No.	1	2	3	4
Sample preparation				
Test portion	15–30 mg	10–20 mg for soil RMs	~ 5 mg	3–100 mg
		500 mg for ERM-CD281		
Pre-treatment	–	calcination 450 °C	calcination 450–500 °C	–
Decomposition	NaOH fusion	NaOH fusion	NaOH fusion	NaOH fusion
Cation exchange resin used for Si purification	AG50W-X12	AG50W-X8	AG50W-X12	AG50W-X8
Amount of Si processed through column purification	7.2 µg	20–150 µg	20–40 µg	4–50 µg
Method used to check Si solutions	Spectrophotometer	ICP-MS	ICP-OES	ICP-OES
Amount of Si in procedural blank	< 25 ng Si total	< 30 ng Si total	< 30 ng Si total	< 16 ng Si total
Analysis				
Instrument	Neptune+	Neptune+	Neptune	Neptune Plus
Plasma mode	Wet	Wet	Wet	Semi-dry
Sample introduction	PFA spray chamber	Thermo double pass	Thermo SIS spray	Apex HF (PFA)
		spray chamber	chamber	
Nebuliser	PFA *ca* . 100 µl min^{-1}	PFA *ca* . 100 µl min^{-1}	PFA *ca* . 70 µl min^{-1}	PFA *ca* . 145 µl min^{-1}
Cones	Regular sampler	Regular Ni cones	Regular sampler	Jet sampler
	Ni X skimmer		Ni X skimmer	H skimmer
Amplifier resistor	10^{11} W	10^{11} W	10^{11} W	10^{11} W
Measurement mode	MR	MR	MR–HR	MR
Mg doping	Yes (Si/Mg ~ 1:1)	Yes ($^{28}Si/^{24}Mg$ ~ 1:1)	Yes	Yes (Si/Mg ~ 1:1)
Si conc. used for analysis	~ 3.6 µg/analysis	~ 3 µg/analysis	~ 3 µg/analysis	~ 0.5 µg/analysis
Sensitivity	18–25 V/2–2.5 ppm	10–15 V/2–2.5 ppm	14 V/3 ppm	11 V/0.5 ppm
Typical ^{28}Si intensity during analysis	8 V/ppm ^{28}Si	4–5 V/ppm ^{28}Si	3–4 V/ppm ^{28}Si	*ca* . 20 V/ppm ^{28}Si
Matrix of analysed solution	1% HNO_3	1% HNO_3	0.05 mol l^{-1} HCl	0.1 mol l^{-1} HCl
Measurement standard used for bracketing	NBS 28	NBS 28	NBS 28	NBS 28
Typical instrument blank intensity ^{28}Si	< 0.07 V	< 0.08 V	~ 0.05 V	< 0.02 V
Data acquisition	1 block of 20 analyses	1 block of 36 analyses	1 block of 25 scans	1 block of 30 cycles
	in dynamic mode with	in dynamic mode with	of 8.4 ms	in dynamic mode with
	4 s integration time/	4 s integration time/		4 s integration time/
	cycle	cycle		cycle
Analytical replication procedure	Not consecutive on the	On different days	On the same day, not	On different days
	run; run over several		consecutive on the run	
	days		(except for ERM-CD281	
			ran on different days)	
RMs analysed for quality control in this study				
$d^{30}Si_{NBS28}$ Diatomite (± 2*s*)	+1.20 ± 0.10‰ (n=7)	+1.25 ± 0.10‰ (n=40)	NA	NA
$d^{29}Si_{NBS28}$ Diatomite (± 2*s*)	+0.66 ± 0.07‰ (n=7)	+0.66 ± 0.07‰ (n=40)	NA	NA
$d^{30}Si_{NBS28}$ BHVO-2 (± 2*s*)	NA	-0.25 ± 0.11‰ (n=14)	NA	-0.28 ± 0.02‰ (n=8)
$d^{29}Si_{NBS28}$ BHVO-2 (± 2*s*)	NA	-0.12 ± 0.11‰ (n=14)	NA	-0.15 ± 0.05‰ (n=8)

Table 2 (continued).
Detailed overview of chemical preparation and analytical techniques used by each laboratory

Laboratory	IFREMER	STAiG	WQC
Laboratory No.	5	6	7
Sample preparation			
Test portion	~ 5 mg	~ 10 mg	100–140 mg
Pre-treatment	–	calcination 450 °C	calcination 420 °C
Decomposition	NaOH + Na_2O_2 fusion	NaOH fusion	NaOH fusion
Cation exchange resin used for Si purification	AG50W-X12	AG50W-X12	AG50W-X12
Amount of Si processed through column purification	30–60 µg	20 µg	5 µg
Method used to check Si solutions	MC-ICP-MS	Spectrophotometer	ICP-OES
Amount of Si in procedural blank	< 20 ng Si total	< 35 ng Si total	< 20 ng Si total
Analysis			
Instrument	Neptune	Neptune+	Neptune
Plasma mode	Semi-dry	Wet	Semi-dry
Sample introduction	Apex	Thermo SIS spray	Apex-Q
		chamber	
Nebuliser	PFA *ca*. 100 µl min^{-1}	PFA *ca*. 75 µl min^{-1}	PFA *ca*. 50 µl min^{-1}
Cones	Regular Ni cones	Ni sampler	Ni sampler
		Ni "H" skimmer	Ni "H" skimmer
Amplifier resistor	10^{13} W	10^{11} W	10^{11} W
Measurement mode	MR	MR	MR
Mg doping	Yes	No	No
Si conc. used for analysis	~ 0.5 µg/analysis	~ 1.6 µg/analysis	~ 2 µg/analysis
Sensitivity	30–35 V/2 ppm	18–25 V/2 ppm	12–14 V/ppm
Typical ^{28}Si intensity during analysis	*ca*. 10 V/ppm ^{28}Si	*ca*. 9 V/ppm ^{28}Si	*ca*. 7–9 V/ppm ^{28}Si
Matrix of analysed solution	2% HNO_3	1% HNO_3	2% HNO_3
Measurement standard used for bracketing	in house RM	NBS 28	NBS 28
Typical instrument blank intensity ^{28}Si	< 0.04 V	< 0.1 V	< 0.06 V
Data acquisition	1 block of 25 analyses	1 block of 25 analyses	1 block of 25 analyses
	in dynamic mode with	in static mode with	in dynamic mode with
	4 s integration time/	8 s integration time/	8.1 s integration time/
	cycle	cycle	cycle
Analytical replication procedure	On the same day,	On different days	On different days
	consecutive on the run		
RMs analysed for quality control in this study			
$d^{30}Si_{NBS28}$ Diatomite (± 2*s*)	+1.26 ± 0.17‰ (n=6)	+1.24 ± 0.04‰ (n=4)	NA
$d^{29}Si_{NBS28}$ Diatomite (± 2*s*)	+0.68 ± 0.09‰ (n=6)	+0.64 ± 0.04‰ (n=4)	+0.64 ± 0.05‰ (n=21)
$d^{30}Si_{NBS28}$ BHVO-2 (± 2*s*)	-0.24 ± 0.08‰ (n=6)	-0.32 ± 0.04‰ (n=8)	NA
$d^{29}Si_{NBS28}$ BHVO-2 (± 2*s*)	-0.12 ± 0.06‰ (n=6)	-0.16 ± 0.04‰ (n=8)	-0.14 ± 0.05‰ (n=21)

Test portion refer to the aliquot amount of the original sample taken for analysis.
Typical instrument blank intensity refers to the intensity of ^{28}Si measured in the "Si-free" matrix solution used for sample dilution.
LR and MR refer to the mass resolving power RP, defined as $m/\Delta m = m/[5\% - m/[95\%]$, where m [5%] and m [95%] are the masses at 5% and 95% peak intensity, respectively, and m is the mass of the peak. LR = low RP [> 1000], MR = medium RP [> 6000].
Si sample consumption per analysis included sample take-up/stabilisation and data acquisition.

Table 3.
Means (arithmetic mean), expanded uncertainties (U, k = 2), number of full procedural replicates (N) and total number of measurments (n) for each reference material analysed in this study

	$d^{29}Si_{NBS\,28}$	U, k = 2	N	n	$d^{30}Si_{NBS\,28}$	U, k = 2	N	n
	(‰)	(‰)			(‰)	(‰)		
GBW-07401	-0.15	0.04	18	86	-0.27	0.06	17	78
GBW-07404	-0.38	0.08	17	86	-0.76	0.12	16	79
GBW-07407	-0.92	0.12	18	80	-1.82	0.17	17	72
TILL-1	-0.07	0.05	12	63	-0.16	0.06	11	55
ERM-CD281	-0.13	0.10	12	38	-0.28	0.11	11	34

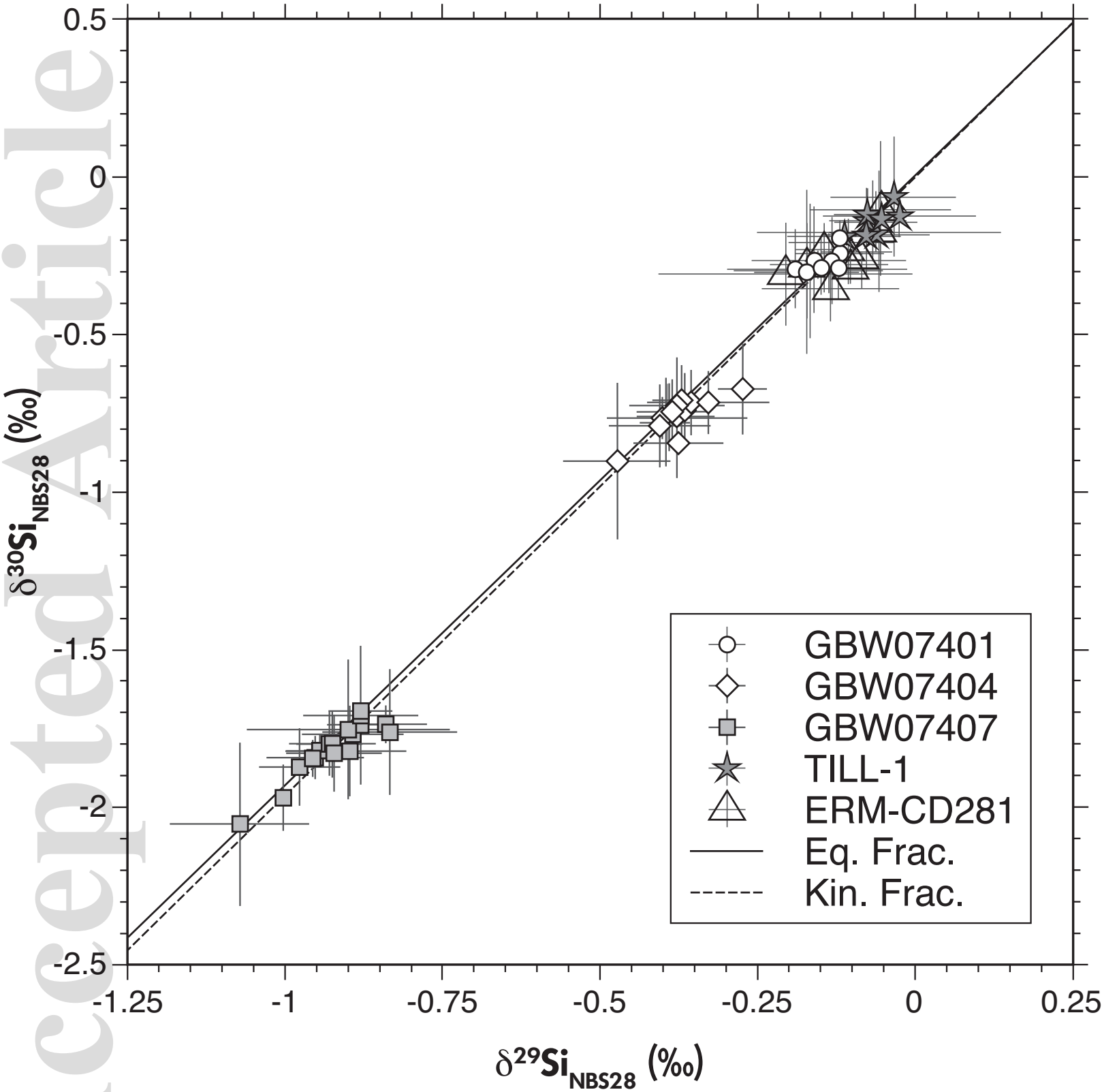

ggr_12378_f1.eps

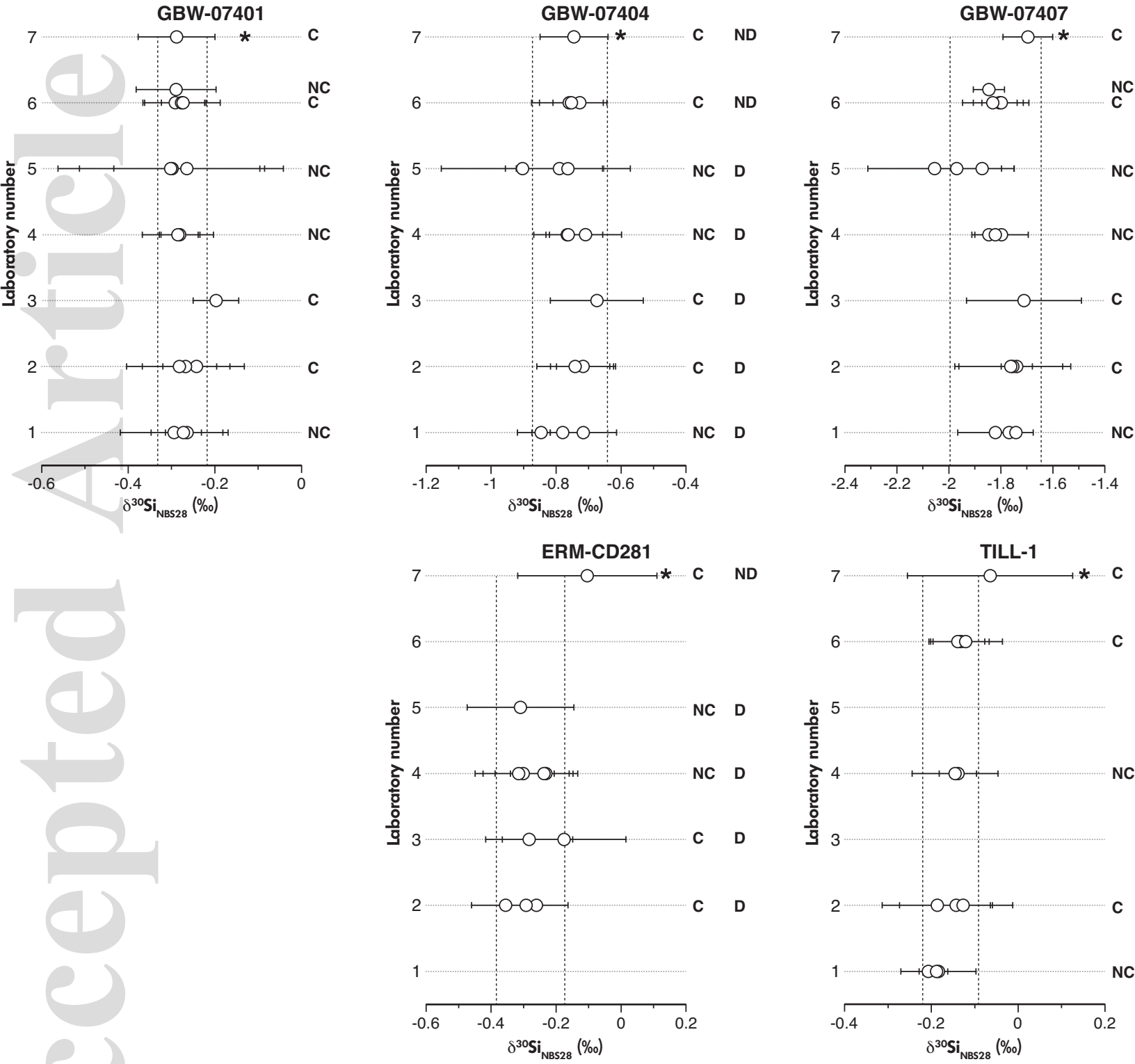

ggr_12378_f2.eps

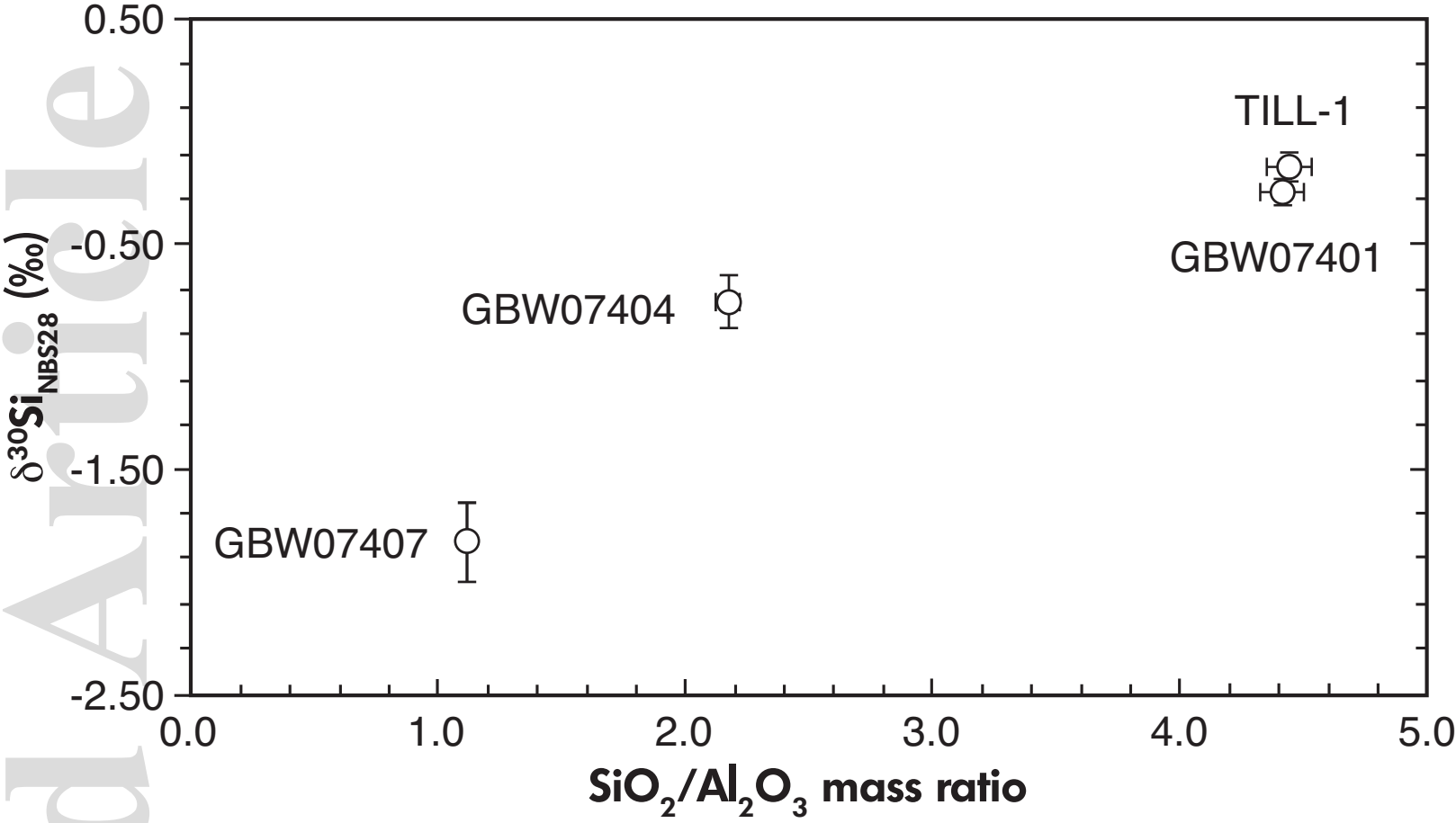

ggr_12378_f3.eps